Performance predictions of one-way energy capture by an oscillating water column device in Faroese waters

Joensen, Bárdur; Bingham, Harry B.; Read, Robert; Nielsen, Kim; Brito Trevino, Jokin

Published in:
Proceedings of the 14th European Wave and Tidal Energy Conference

Publication date:
2021

Document Version
Publisher's PDF, also known as Version of record

Performance predictions of one-way energy capture by an oscillating water column device in Faroese waters.

Bárdur Joensen, Harry B. Bingham, Robert W. Read, Kim Nielsen, and Jokin Brito Trevino

***Abstract*—Here we investigate the performance of an experimentally tested model-scale oscillating water column (OWC) device, modified to only exploit half of the wave cycle. To do this we integrate a passive valve system into the OWC chamber which ensures a free connection to the atmosphere either on the up- or the down-stroke, but sends the flow through the orifice plate representing the full-scale air turbine, on the other half-cycle. The performance of the experimental model is evaluated from the absorbed power of the OWC chamber. The absorbed power is computed from the measured pressure drop across an orifice plate and the internal surface elevation inside the chamber. Perhaps surprisingly, the device can absorb more energy near resonance when exploiting only half of the cycle than when the full cycle is exploited. Since a one-way turbine is typically much more efficient than a Wells, impulse, bi-radial, or other self-rectifying turbine, this suggests a significant potential gain in overall efficiency from wave to wire. The obtained performance characteristics of the model-scale device are extrapolated to a proposed full-scale device size, and its performance is evaluated in Faroese waters. The performance of the proposed full-scale device is presented in terms of the annual absorbed power.**

***Index Terms*—Wave power, Oscillating Water Column, One-way energy capture**

I. Introduction

As the world's energy demand increases, together with the increased awareness of the harmful effects of carbon emissions, we as a world society must move quickly to replace fossil-fuel based energy production with renewable energy sources. Ocean waves are a potential candidate for significant renewable energy supply. There exist several different working principles to convert energy from waves to electrical energy. One of the more promising technologies is the oscillating water column (OWC) wave energy converter (WEC). The OWC has the attractive feature, of having no moving parts submerged in water, albeit having a reduced conversion efficiency from wave-to-wire when using a conventional Wells turbine.

Much effort has been invested in research and development of OWC type wave energy converters [1]. The conventional configuration of an OWC device uses a self-rectifying turbine as the power take off (PTO) system [2]. Many different types of configurations have been investigated to improve the efficiency of OWC devices. For example the LEANCON device [3], is a V-shaped structure, consisting of several OWC chambers on each arm of the V-shape. The OWC chambers are connected by non-return valves to two ducts which feed a unidirectional turbine.

Another concept is the Tupperware device, which is a closed circuit machine equipped with one high-pressure chamber and one low-pressure chamber connected by a unidirectional air turbine. Benreguig et. al. [4] performed a study comparing two different numerical models with experimental results. The first numerical model uses ODEs coupling hydrodynamic and thermodynamic variables. It is based on linear potential flow theory and solves the Cummins equation [5]. The second numerical model is a Computational Fluid Dynamics (CFD) model based on the Reynolds Averaged Navier-Stokes (RANS) equations.

Another concept currently under development is the UniWave OWC wave energy device, developed by WaveSwell Energy [6]. Fleming et. al. [7] conducted model-scale experiments to investigate the power performance of the UniWave concept wave energy converter. Ansarifard et. al. [8] performed a numerical investigation using CFD to analyse a unidirectional radial air-inflow-turbine design for the UniWave wave energy converter.

The present study is based on the KNSwing concept, an attenuator type wave energy converter. The KNSwing model is a ship like structure equipped with 20 oscillating water column chambers on each side [9]. However, this study only focuses on the experimental performance of one fixed oscillating water column chamber, whereas the numerical calculations are presented for both a single OWC device and the full 40-chamber device. In the experiments, the OWC chamber opening is oriented along the incoming wave crests, thus rotated 90 degrees compared to Fleming et. al. [7]. It is furthermore equipped with a passive, low-inertia non-return valve system, to incorporate a unidirectional air turbine power take-off system.

This paragraph of the first footnote will contain the ID number of your paper submission and the conference track where the paper was submitted. This work was supported by the Faroese Research Foundation under grant number 02010. The work was also supported by SEV and Betri Bank.

Bárdur Joensen is with LBF Consulting Engineers, Niels Finsens Gøta 10, 110 Tórshavn, Faroe Islands (e-mail: baj@lbf.fo). He is furthermore enrolled as a Ph.D. student at the Technical University of Denmark (DTU), Department of Mechanical Engineering, Section for Fluid Mechanics, Coastal and Maritime Engineering, Nils Koppels Allé 403, 2800 Kongens Lyngby (e-mail: bajoe@mek.dtu.dk).

Harry B. Bingham (hbb@mek.dtu.dk) and Robert Read (rrea@mek.dtu.dk) are with the Department of Mechanical Engineering, Section for Fluid Mechanics, Coastal and Maritime Engineering, at the Technical University of Denmark.

Kim Nielsen (kin@ramboll.com) and Jokin Brito Trevino (jnbo@ramboll.dk) are with Rambøll A/S, Hannemanns Allé 53, 2300 Copenhagen S.

II. Hydrodynamic theory

As the hydrodynamic theory regarding the numerical analysis of the OWC chamber has been thoroughly explained in [10] and [11], we will here briefly summarize the theory and present the equations used to compute the relevant results.

The total volume flux through the chamber is given by:

$$q = \int_{S_i} \partial_z \phi \, \mathrm{d}S = \int_{S_i} \partial_z \phi_D \, \mathrm{d}S + \int_{S_i} \partial_z \phi_R \, \mathrm{d}S = q_D + q_R \tag{1}$$

where the subscript D stands for diffraction, the subscript R stands for radiation, with ϕ the velocity potential and ∂_z indicating a partial derivative with respect to the vertical coordinate z. Here S_i is the interior chamber free surface. The radiation and diffraction potentials are computed as described by [10]. The mean power extracted by the turbine over one period of oscillation is given by

$$W = \frac{1}{T}\int_0^T \Re\{p\mathrm{e}^{\mathrm{i}\omega t}\}\Re\{q\mathrm{e}^{\mathrm{i}\omega t}\}dt = \frac{1}{2}\Re\{p^* q\} \tag{2}$$

where p^* is the complex conjugate of p, the applied pressure from the turbine or orifice plate, and $T = 2\pi/\omega$ is the wave period. Generally speaking, there is a quadratic relation between the volume flux through the orifice and the pressure drop across the orifice. However, for a weakly-nonlinear, frequency-domain solution, we assume a linear relation between the flux and the pressure in each chamber. The flux is given by

$$q = \mathrm{i}\omega A_c \xi \tag{3}$$

with A_c the free surface area of the chamber, and ξ the mean chamber response phasor. Denoting B_0 as the equivalent linearized damping coefficient of the orifice plate, the pressure becomes

$$p = -\mathrm{i}\omega B_0 \xi / A_c. \tag{4}$$

If we have N_c total chambers, the total mean power extracted by the device over one cycle of oscillation is then

$$W = \sum_{n=1}^{N_c} \frac{1}{2}\omega^2 B_{n0} \xi_n^* \xi_n, \tag{5}$$

where B_{n0} and ξ_n are the damping coefficient and mean chamber response for the n^{th} chamber.

The total power extracted will normally be expressed as a capture width ratio by scaling it with the maximum available power passing through a section of the free-surface of length L_c along a wave crest

$$W_{max} = \frac{1}{2}\rho g A^2 c_g L_c, \tag{6}$$

where L_c is taken as the body length, A is the wave amplitude, c_g is the wave group velocity, and ρ, g are respectively the water density and the gravitational acceleration. In terms of the absorbed power of the device and the maximum available power resource, the capture width ratio can be written as

$$\overline{W} = \frac{W}{W_{max}}. \tag{7}$$

The air turbine used to extract power from the OWC is modelled in the lab by forcing the air through an orifice in the chamber roof, which has an area of approximately 1% of the internal free surface area. Ignoring compressibility effects, which are usually negligible at model scale, the pressure drop across the orifice is proportional to the square of the volume flux through the orifice

$$p(t) = \frac{1}{2}\rho_a \left(\frac{1}{C_d a}\right)^2 Q(t)^2 \mathrm{sign}(Q) = R_0 Q(t)^2 \mathrm{sign}(Q) \tag{8}$$

where ρ_a is the air density, a is the orifice area and C_d is an effective area coefficient, experimentally determined to be $C_d = 0.64$ for the chamber and orifice used here.

To estimate an equivalent linear damping coefficient, we assume an oscillatory flux in the chamber as

$$Q(t) = |q|\sin(\omega t) \tag{9}$$

and find the B_0 which gives the same mean power loss over one cycle of oscillation. This gives

$$B_0 = \frac{8}{3\pi}\omega A_c R_0 |\xi| \tag{10}$$

as the relation between the linear and nonlinear damping coefficients. Since the mean chamber response amplitude $|\xi|$ appears in this relation, the solution must be found iteratively at each frequency ω and each wave steepness A/L, where L is the wavelength. This makes the equations weakly nonlinear.

For one-way energy capture, when the turbine works only over half of the cycle, the nonlinear power is divided by two and the relation becomes

$$B_0 = \frac{4}{3\pi}\omega A_c R_0 |\xi|. \tag{11}$$

In the context of this simplified, weakly-nonlinear model, there is no difference between venting on the upstroke and venting on the downstroke.

III. Experimental work

A. Experimental setup

The experimental work discussed here is the result of a measurement campaign carried out in Flume 1 in the Hydraulics Laboratory at the Technical University of Denmark (DTU). Flume 1 measures 25 by 0.6 metres with a water depth of 0.65 m. It is equipped with a piston-type wavemaker at one end, and an absorbing beach at the opposite end. The internal chamber of the model measures 0.12 m by 0.1 m. As the flume is quite narrow compared to the width of the internal chamber, it is expected to see some wall effects. For the relationship between the full scale prototype and the model scale experimental model, Froude similarity is ensured.

The performance of the OWC model chamber device (Fig. 1) was tested for a series of 30 mono-chromatic waves, with two wave height to wavelength ratios H/L =0.025 and H/L =0.04.

The fixed OWC chamber was placed near the middle of the flume, at a distance of 12.35 m from the wavemaker, see Fig. 2. The internal surface elevation

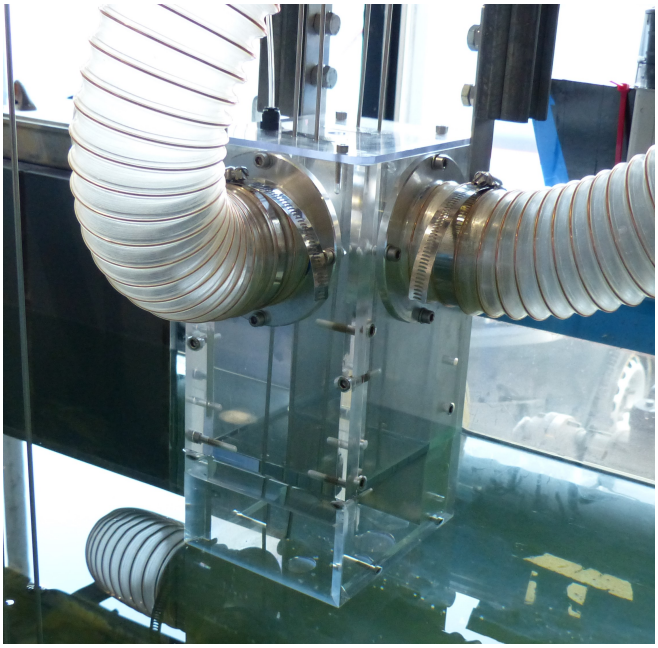

Fig. 1. Picture of the OWC chamber.

of the OWC is measured using resistance-type wave gauges from Edinburgh Designs [12]. Together with the internal surface elevation, the pressure drop across the orifice is measured using a differential pressure sensor, from First Sensor [13].

In contrast to conventional OWC configurations, we here use a valve system, to only exploit half of the wave cycle. This means that as the waves pass by the chamber, the air inside the chamber is let out of the chamber with minimal resistance, on either the up-stroke or down-stroke of the wave cycle. A detailed description of the valve system can be found in [14].

B. Analysis of experimental data

As mentioned in the preceding section, the internal surface elevation in the chamber was measured using two resistance-type wave probes. The mean internal surface elevation $\eta(t)$, together with the internal chamber surface area S, are used to compute the volume flux through the orifice as a function of time,

$$Q(t) = \frac{d\eta}{dt} S. \tag{12}$$

The volume flux together with the measured pressure drop across the orifice is used to compute the absorbed power as

$$W(t) = Q(t)\, p(t), \tag{13}$$

where the mean absorbed power is computed as

$$W = \frac{1}{T} \int_0^T W(t) dt. \tag{14}$$

The experimentally determined absorbed power is divided by the maximum available power from (6) to give the capture width ratio. As we here look at a double chamber section, the absorbed power is multiplied by two, while the maximum available power stays unchanged, since the length along the wave crest remains the same.

C. Harmonic analysis

To analyse the measured signals from the wave- and pressure gauges, a clean periodic signal is necessary. Therefore, a harmonic analysis is performed on the measured signal. The harmonic analysis uses a least-squares fitting method, which estimates the analysed signal as a sum of time-varying sinusoids at frequencies that are multiples of the fundamental frequency, plus a mean value.

IV. Results

The two aforementioned configurations of the experimental set up of the valve system - venting on the up-stroke cycle of the wave and venting on the down-stroke of the wave cycle are compared with experimental results from an earlier study [11] on the same chamber, but with a conventional two-way configuration.

Fig. 3 shows the absorbed power W of the OWC chamber in Watts as a function of wave period T in seconds, for the two wave steepnesses, $H/L = 0.025$ and $H/L = 0.04$, for the upstroke venting configuration.

Fig. 4 shows the absorbed power of the OWC chamber in Watts as a function of wave period, for the two wave steepnesses, for the downstroke venting configuration.

Fig. 5 shows the normalised absorbed power of the OWC chamber, computed as a function of the wave period for the upstroke venting configuration.

Fig. 6 shows the normalised absorbed power of the OWC chamber, computed as a function of the wave period for the downstroke venting configuration.

A. Evaluation of the 40-chamber device in Faroese waters

In order the evaluate the performance of the OWC device, we here look at the numerically computed capture width ratio of the full 40-chamber device. We use the same analysis procedure as in [15]. The wave data used in the performance evaluation is taken from [16], as is done in [15]. The average absorbed power is computed as follows:

$$P_{abs(SS)} = \rho g L_c \int_0^\infty c_g(\omega) S(\omega) \overline{W}(\omega)\, \mathrm{d}\omega \tag{15}$$

where the capture width ratio is given by (7), and S is the wave spectral energy density computed using the WAFO toolbox, see [17]. The absorbed power is multiplied by the probability of occurrence of each sea-state P_r, and summed to give the total absorbed power, as

$$P_{abs(tot)} = \sum_{SS=1}^{N} P_{abs(SS)}\, P_r. \tag{16}$$

For simplicity's sake, we choose here to only look at the 2.5% wave steepness case. Furthermore, from the numerically computed capture width ratio, we choose to investigate the effect of slightly altering the orifice diameter. By changing the orifice diameter, and thereby the damping, this might have a positive or negative effect on the performance of the wave energy device.

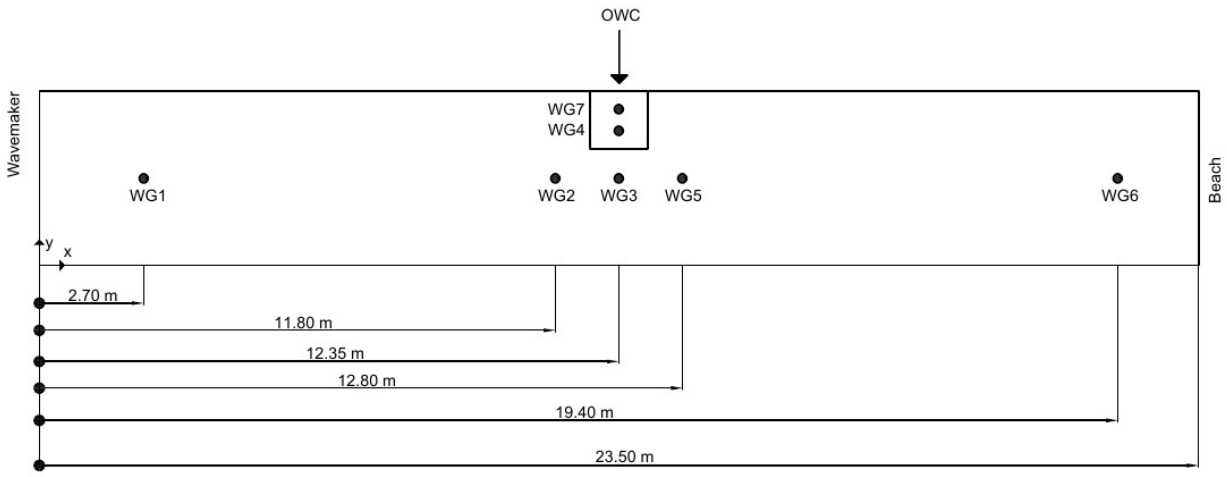

Fig. 2. Sketch of the wave tank used in the experiments. 'WG' is an abbreviation for wave gauge.

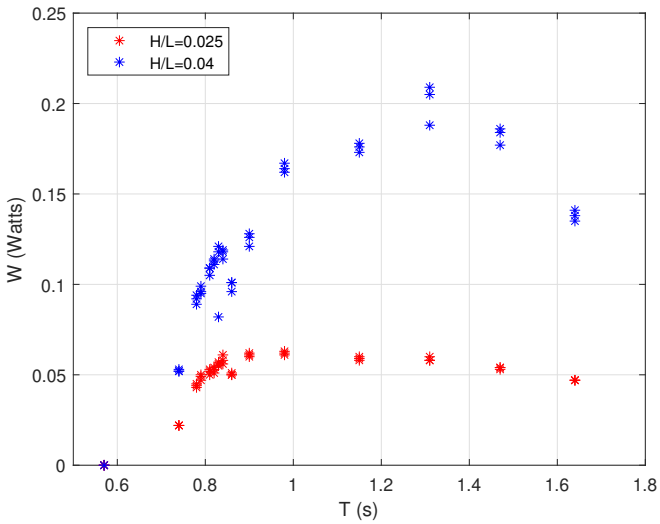

Fig. 3. Experimentally measured absorbed power, upstroke venting configuration.

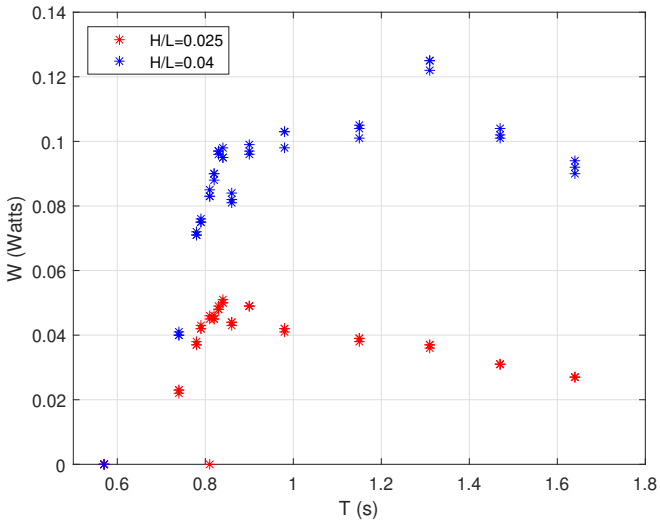

Fig. 4. Experimentally measured absorbed power, downstroke venting configuration.

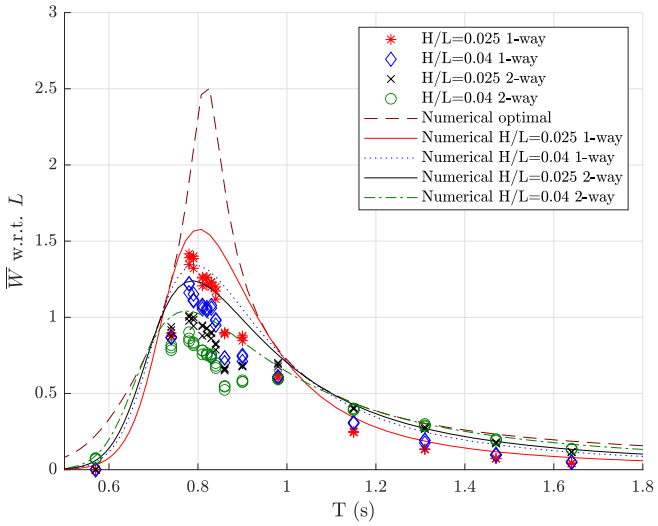

Fig. 5. Numerical calculations compared with experimental data. Here the upstroke venting of the chamber (1-way) is compared with the two-way energy capture (2-way) of the chamber.

TABLE I
THE TWO CONSIDERED LOCATIONS.

Site	Lat/Long	Depth	Avg. P	Dist. to shore
[-]	[deg]	[m]	[kW/m]	[m]
E1	61.8/-6.6	41	11	1680
W1	61.8/-6.9	61	40	628

Fig. 7 shows the numerically computed capture width ratio for three steepness values - 2.5%, 4% and 6%. The figure shows that the non-dimensional absorbed power of the lowest wave steepness is highest.

Fig. 8 shows the capture width ratio at wave steepness 2.5% for five different values of the full-scale orifice diameter d. The figure shows that smaller orifice diameters result in a lower peak capture width ratio. While for the higher values the curve becomes narrower and with a higher peak at near resonance conditions.

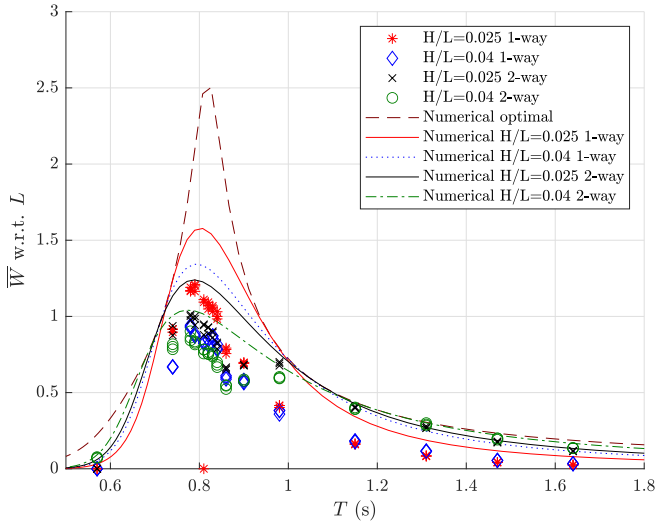

Fig. 6. Numerical calculations compared with experimental data. Here the downstroke venting of the chamber (1-way) is compared with the two-way energy capture (2-way) of the chamber.

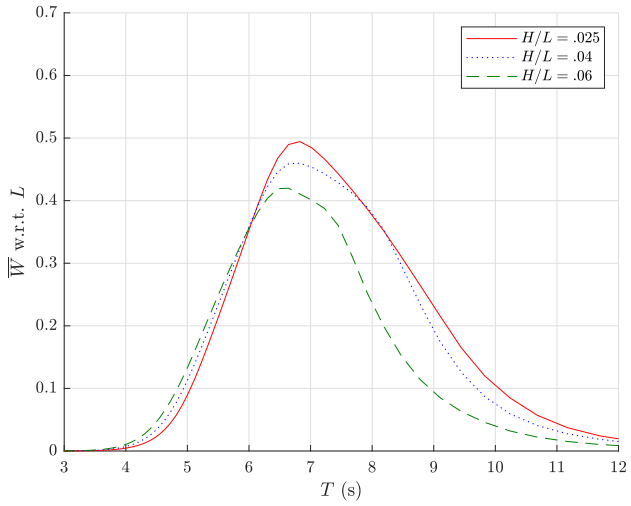

Fig. 7. Numerically computed capture width ratio of the one-way energy capture of the full scale 40 chamber structure for 3 steepness values.

In tables II to VI the absorbed power in kW is shown for two sites considered in [15]. These two site locations are considered to be representative for the east- and west coast of the Faroe Islands, respectively. The tables show a variation of the length of the structure considered, together with a fixed orifice diameter.

TABLE II
AVERAGE ABSORBED POWER IN KW FOR 2009-2018 AT THE WEST (W1) AND EAST (E1) SITE FOR DIFFERENT SIZES OF THE STRUCTURES WITH FULL SCALE ORIFICE DIAMETER OF D=600MM.

	Length of structure [m]			
	150	300	450	600
W1	**720**	**2775**	**4110**	**4380**
E1	**280**	**485**	**435**	**315**

In tables II to VI it is seen, that there is a vast difference between the east and west site locations, as is seen for the concepts considered in [15]. Furthermore, by increasing the size of the structure, more power is absorbed. However, when increasing from 450 m to 600 m at the W1 site there is little gain in absorbed power. For the E1 site there is actually a decrease in absorbed power when increasing from 300 m to 450 m. The same trend is also seen in [15].

The normalised absorbed power in Figs. 5 and 6 show that the highest efficiency occurs around reso-

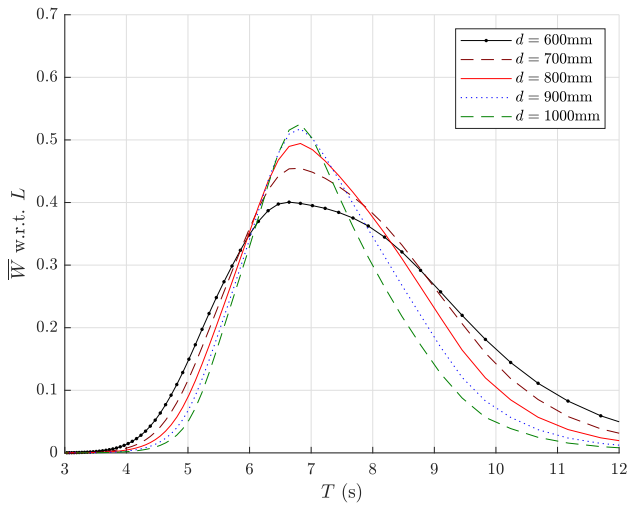

Fig. 8. Numerically computed capture width ratio for 2.5% wave steepness, for five different values of the orifice diameter.

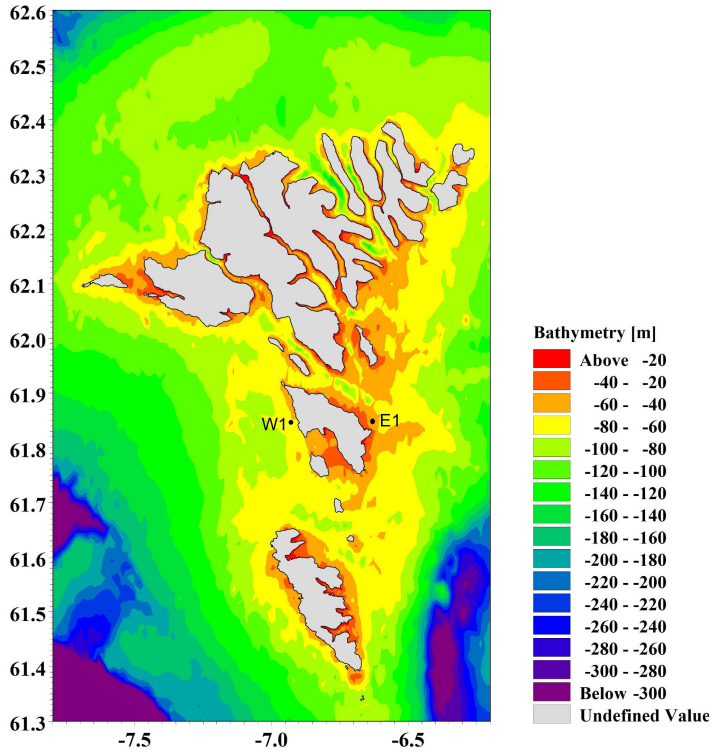

Fig. 9. The two considered locations.

TABLE III
AVERAGE ABSORBED POWER IN KW FOR 2009-2018 AT THE WEST (W1) AND EAST (E1) SITE FOR DIFFERENT SIZES OF THE STRUCTURES WITH FULL SCALE ORIFICE DIAMETER OF D=700MM.

	Length of structure [m]			
	150	300	450	600
W1	**685**	**2875**	**4285**	**4430**
E1	**285**	**495**	**420**	**285**

TABLE IV
AVERAGE ABSORBED POWER IN KW FOR 2009-2018 AT THE WEST (W1) AND EAST (E1) SITE FOR DIFFERENT SIZES OF THE STRUCTURES WITH FULL SCALE ORIFICE DIAMETER OF D=800MM.

	Length of structure [m]			
	150	300	450	600
W1	**610**	**2800**	**4270**	**4340**
E1	**275**	**485**	**395**	**260**

TABLE V
AVERAGE ABSORBED POWER IN KW FOR 2009-2018 AT THE WEST (W1) AND EAST (E1) SITE FOR DIFFERENT SIZES OF THE STRUCTURES WITH FULL SCALE ORIFICE DIAMETER OF D=900MM.

	Length of structure [m]			
	150	300	450	600
W1	**530**	**2620**	**4120**	**4170**
E1	**255**	**465**	**375**	**235**

TABLE VI
AVERAGE ABSORBED POWER IN KW FOR 2009-2018 AT THE WEST (W1) AND EAST (E1) SITE FOR DIFFERENT SIZES OF THE STRUCTURES WITH FULL SCALE ORIFICE DIAMETER OF D=1000MM.

	Length of structure [m]			
	150	300	450	600
W1	**455**	**2390**	**3890**	**3950**
E1	**230**	**440**	**350**	**215**

nance. However, this does not necessarily mean that the most power is absorbed at these conditions. Considering Figs. 3 and 4, the absorbed power is actually higher for the longer waves, i.e. away from resonance conditions. Also, from Fig. 8 it is evident that changing the orifice diameter changes the characteristics of the absorbed power. For smaller orifice diameters the normalised power curve becomes broader, with a lower peak at resonance, while the larger diameters yield a narrower curve with a higher peak. Thus the orifice diameter (which relates to the designed behaviour of the air turbine) can be used to optimise the device to a particular expected yearly distribution of wave climate.

V. CONCLUSIONS

In this paper we present experimental results, together with numerical calculations for a relatively new, one-way energy absorption, configuration of an OWC wave energy device. Results show that at resonance conditions, the normalised absorbed power of the one-way energy configuration is higher compared to the two-way configuration, especially when venting on the upstroke. Furthermore, we present numerical results for the full-scale KNSwing device and the effect of different wave steepness and different orifice diameters. Lastly, we present results for four different proposed full scale sizes for the absorbed power of the devices at two different locations in the Faroe Islands. Here it was seen that the size of the orifice diameter had a large impact on the average absorbed power of the device. This implies that a careful site investigation is necessary when considering device deployment.

ACKNOWLEDGEMENT

This study is part of a Ph.D. project "Wave energy conversion in the Faroe Islands" supported by the Research Council of the Faroe Islands grant number 02010. The project is also financially supported by SEV and Betri Bank.

REFERENCES

[1] A. F. Falcão and J. C. Henriques, "Oscillating-water-column wave energy converters and air turbines: A review," *Renewable Energy*, vol. 85, pp. 1391–1424, jan 2016.

[2] A. F. Falcão, J. C. Henriques, and L. M. Gato, "Self-rectifying air turbines for wave energy conversion: A comparative analysis," *Renewable and Sustainable Energy Reviews*, vol. 91, pp. 1231–1241, aug 2018.

[3] J. P. Kofoed and P. Frigaard, "Hydraulic evaluation of the LEANCON wave energy converter," Aalborg University, Department of Civil Engineering, Tech. Rep., 2008.

[4] P. Benreguig, M. Vicente, A. Dunne, and J. Murphy, "Modelling approaches of a closed-circuit OWC wave energy converter," *Journal of Marine Science and Engineering*, vol. 7, no. 2, p. 23, jan 2019.

[5] W.E. Cummins, "The impulse response function and ship motion," *Schiffstecknik*, vol. 9, pp. 101–109, 1962.

[6] Wave Swell Energy, "https://www.waveswell.com/," [accessed 23.03.2021].

[7] A. Fleming, G. MacFarlane, S. Hunter, and T. Denniss, "Power performance prediction for a vented oscillating water column wave energy converter with a unidirectional air turbine power take-off," in *Proceedings of the 12th European Wave and Tidal Energy Conference*, 2017.

[8] N. Ansarifard, S. Kianejad, A. Fleming, and S. Chai, "A radial inflow air turbine design for a vented oscillating water column," *Energy*, vol. 166, pp. 380–391, jan 2019.

[9] K. Nielsen and H. Bingham, "MARINET experiment KNSWING testing an I-Beam OWC attenuator," *International Journal of Marine Energy*, vol. 12, pp. 21–34, dec 2015.

[10] H. B. Bingham, Y.-H. Yu, K. Nielsen, K.-H. Kim, S. Park, K. Hong, H. A. Said, T. Kelly, J. Ringwood, R. W. Read, E. Ransley, S. Brown, and D. Greaves, "Ocean energy systems wave energy modelling task 10.4: Numerical modelling of a fixed oscillating water column," *Energies*, vol. 14, no. 6, p. 1718, 2021.

[11] H. B. Bingham, D. Ducasse, K. Nielsen, and R. Read, "Hydrodynamic analysis of oscillating water column wave energy devices," *Journal of Ocean Engineering and Marine Energy*, vol. 1, no. 4, pp. 405–419, jul 2015.

[12] Edinburgh Designs, *Wave Gauge Software Manual*, 2018.

[13] First Sensor, *BTEL/PTUL5000 Series*, 2008.

[14] B. Joensen, H. B. Bingham, R. Read, K. Nielsen, and J. B. Trevino, "Hydrodynamic analysis of a one-way energy capture of an oscillating water column wave energy device," *(In preparation)*, 2021.

[15] B. Joensen, H. B. Bingham, and B. A. Niclasen, "Evaluation of the power performance of various wave energy conversion concepts for Faroese coastal waters," in *Developments in renewable energies offshore*. CRCPress/Balkema, 2021, pp. 96–102.

[16] B. Joensen, B. A. Niclasen, and H. B. Bingham, "Wave power assessment in Faroese waters using an oceanic to nearshore scale spectral wave model," 2020, manuscript submitted for publication.

[17] WAFO-group, *WAFO - a matlab toolbox for analysis of random waves and loads - a tutorial.*, Math. Stat., Center for Math. Sci., Lund Univ., Sweden., 2017. [Online]. Available: http://www.maths.lth.se/matstat/wafo/documentation/index.html